Floquet poor man's Majorana fermions in double quantum dots

Yantao Li,* Yankui Wang, and Fan Zhong†
State Key Laboratory of Optoelectronic Materials and Technologies, School of Physics and Engineering, Sun Yat-sen University, Guangzhou 510275, People's Republic of China
(Dated: January 17, 2013)

We consider a system consisting of two quantum dots connected by an s-wave superconductor in the presence of periodically varying electric or magnetic fields. The Floquet theory shows that there may be Floquet poor man's Majorana fermions (FPMMFs) in the high frequency region depending on the phase difference between the applied external fields to the two dots. Numerical results confirm this expectation and find in addition a lot of FPMMFs in the low frequency region. The FPMMFs survive for nonzero energy levels of the two dots and their interaction though the frequencies at which they emerge change and thus may be a promising candidate to be detected in experiments.

PACS numbers: 74.45.+c, 85.35.Gv, 74.20.Mn

I. INTRODUCTION

Recent researches on Majorana's fermion whose antiparticle is itself bring exciting new physics in the fields of condensed matter physics and ultracold atoms,[1–3] especially the Majorana fermion observed in the very recent experiments.[4–8] However, to definitely confirm the observed Majorana fermion, one still needs more careful analysis and other promising experiments, since factors such as disorder can also induce the experimentally observed zero-bias anormaly in differential conductance.[9] Therefore, many other promising designs for detecting the Majorana fermion have been proposed.[10,11] Among them, instead of quantum wires one can use quantum dot array to host Majorana bound state for the reason that the latter can overcome the disorder effects efficiently.[12,13] Besides, easily-controlled quantum dots not only can be used for the detection of Majorana fermions in quantum wires,[14] but also may be helpful for non-Abelian statistics realizations.[15]

On the other hand, similar to Floquet topological insulators,[16] there is also a line to study the topological superconductor system by periodically driving the chemical potential or external fields. The concept of Floquet Majorana fermions was introduced in the ultracold atoms.[17] This line becomes more and more attractive,[18–20] since the rich physics may appear in the periodically changed systems such as nonzero energy Majorana fermions in the Floquet space based on the fact that states can keep intact when Floquet quasienergies change by integral multiples of frequency ($\hbar$ is set to unit in this paper). Also, it has been pointed out that Floquet Majorana fermions follow the same statistics properties as ordinary ones.[21]

In this paper, we introduce Floquet poor man's Majorana fermions and study their properties on the basis of the very recently proposed interesting work of poor man's Majorana fermions (PMMFs).[24] The PMMFs share the same properties as the ordinary Majorana fermions, but lack topological protection. The PMMFs are so interesting because not only their detection is very feasible as there were already other experiments on the very similar systems,[22,23] but also they can locate at the double quantum dots separate without overlapping with each other.

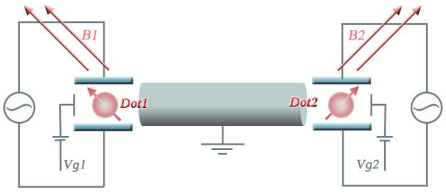

FIG. 1. (Color online) Schematic diagram of two quantum dots connected by an s-wave superconductor. The gates V_{g1} and V_{g2} tune the energy levels of the double dots. The magnetic fields B_1 and B_2 fix the spin directions of the electrons and provide nonzero values of Δ and λ (see text). Two alternating circuits with local electrodes are connected to the dots to produce periodically varying chemical potentials.

In the following, we first introduce the system we considered in Sec. II and recall the condition of the appearance of PMMF in Sec. III. Then we describe in Sec. IV how to use the Floquet theory to analyse the appearance of FPMMF when the adiabatic approximation is met. Sec. V concentrates on numerical studies. We first calculate in Sec. V A the quasienergy and Floquet modes in the absence of interaction both in the low frequency and high frequency region in the Nambu space, even the adiabatic approximation is violated. Then, we transfer from the Nambu space to the Fock Space to consider the interaction effects in Sec. V B. The time evolution of Floquet modes is presented in Sec. V C followed by a summary in Sec. VI.

II. MODEL

The system we considered is illustrated in Fig. 1, the double quantum dots are connected by an s-wave superconductor. We assume for simplicity that there is only one state in each quantum dots, and the spin directions of the electrons are fixed by their respective magnetic fields B_1 and B_2. As a result, no double occupancy and intra-dot electron interactions exist and only the interac-

tion between the dots is considered. The Hamiltonian of the system is then,

$$H = \epsilon_1 d_1^\dagger d_1 + \epsilon_2 d_2^\dagger d_2 + U d_1^\dagger d_1 d_2^\dagger d_2 + \lambda \left(d_1^\dagger d_2 - d_1 d_2^\dagger \right) + \Delta \left(d_1^\dagger d_2^\dagger - d_1 d_2 \right), \quad (1)$$

where $d_i^\dagger$ and d_i are the creation and annihilation operators of electrons in dot i with the energy levels ϵ_i $(i = 1, 2)$, respectively, U is the interaction between the electrons, λ is the co-tunneling hopping amplitude, and Δ represents the amplitude of cross Andreev reflections. The driving term produced by the electric or magnetic field is,

$$H_e(t) = \mathbf{f}_1(t) d_1^\dagger d_1 + \mathbf{f}_2(t) d_2^\dagger d_2, \quad (2)$$

where $\mathbf{f}_1 = A\cos(\omega t)$ and $\mathbf{f}_2 = A\cos(\omega t + \vartheta)$, ω is the driving frequency, t is the real time, A and ϑ are the driving amplitude and the phase difference. Note that the forms of the contributions of the electric field and magnetic field to the Hamiltonian are identical and the driven terms change in fact the chemical potential. However, it is more easy to use the electric field in practical experiments as it is more easy to be controlled.

III. POOR MAN'S MAJORANA FERMIONS

We recall briefly in this section how the PMMFs appear in such a system in Leijnse and Flensberg's paper.[24] In their work, an inhomogeneous magnetic field are applied to modify the values of Δ and λ: $\Delta = \Delta_0 \sin(\theta/2)$, $\lambda = \lambda_0 \cos(\theta/2)$, with θ being the angle between the the directions of magnetic fields applied on the two dots. Tuning the angle can then make the ratio Δ/λ equal unit. At this ratio, the solution of the Hamiltonian has two degenerated zero eigenvalues. The corresponding eigenstates are two well separated Majorana bound states: $\gamma_1 = (d_1 + d_1^\dagger)/\sqrt{2}$ and $\gamma_2 = i(d_2 - d_2^\dagger)/\sqrt{2}$. γ_1 locates in dot 1 and γ_2 locates in dot 2. Thus tuning the ratio is one of the key points in forming Majorana bound states in the system. We shall show in the following how to tune the ratio using periodically varying external fields and reveal rich phenomena in this case.

IV. ANALYTICAL RESULTS IN HIGH FREQUENCIES

Let us introduce Floquet's theory[25,26] which is a theory to handle a system whose Hamiltonian is periodically changed in time. According to this theory, for $H(t+T) = H(t)$ with a period $T = 2\pi/\omega$, the wave function $|\psi(t)\rangle$ of the Schrödinger equation,

$$H|\psi(t)\rangle = i\frac{\partial}{\partial t}|\psi(t)\rangle, \quad (3)$$

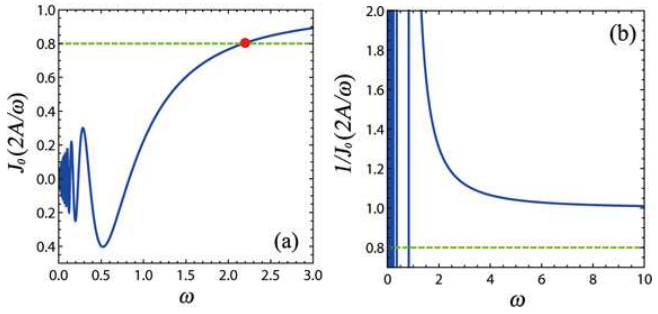

FIG. 2. (Color online) (a) Zero-order Bessel function and (b) its inverse as a function of frequency. In the high frequency region, a pair of FPMMFs appears (red circle) at the phase difference $2k\pi$ in (a), and the pair of FPMMFs disappears at the phase difference $(2k+1)\pi$ in (b). We set $A = 1$ and the fixed ratio $\lambda/\Delta = 0.8$.

can be expressed as

$$|\psi_\alpha(t)\rangle = \exp(-i\varepsilon_\alpha t)|\varphi_\alpha(t)\rangle, \quad (4)$$

where ε_α is the quasienergy and $|\varphi_\alpha(t)\rangle$ is the periodic Floquet state satisfying $|\varphi_\alpha(t+T)\rangle = |\varphi_\alpha(t)\rangle$. Substituting this into Eq. (3), one obtains the Floquet equation,

$$H_f|\varphi_\alpha(t)\rangle = \varepsilon_\alpha|\varphi_\alpha(t)\rangle \quad (5)$$

with the Floquet Hamiltonian being defined as $H_f = H - i\partial/\partial t$. One can also use the time evolution operator $U(t_0+T, t_0) \equiv \mathbb{T}\exp(-i\int_{t_0}^{t_0+T} H(t)dt)$ to express the Floquet equation as

$$U(t_0+T, t_0)|\varphi_\alpha(t_0)\rangle = \exp(-i\varepsilon_\alpha T)|\varphi_\alpha(t_0)\rangle, \quad (6)$$

where $\mathbb{T}$ is the time order operator. Solving the Floquet equation instead of the original Schrödinger equation is the way of the Floquet theory to handle the nonequilibrium problem. This is similar to the Bloch theory which handles a system with periodically changed Hamiltonian in space. Thus to diagonal the Floquet Hamiltonian is the main task for obtaining the quasienergy and the Floquet state.

To this end, we use the rotating wave approximation,[27]

$$|\{n_i\}, m\rangle = \exp\left(im\omega t - i\int_0^t H_e(t')dt' \right)|\{n_i\}\rangle, \quad (7)$$

to express the Floquet state, where $t_0 = 0$, $|\{n_i\}\rangle$ means a state in Fock space and the integer m is the quantum number of the so-called photon mode in the space. Absorbing or emitting a photon can be compensated by adding or removing a quasienergy equal to the photon energy without changing the wave function of the original Schrödinger equation from Eq. (4). To ensure the orthogonality of the Floquet states, one should define the inner product of the Floquet states over a period besides the traditional inner product, viz.

$$\langle\langle\varphi_\alpha(t)|\varphi_\beta(t)\rangle\rangle \equiv \frac{1}{T}\int_0^T \langle\varphi_\alpha(t)|\varphi_\beta(t)\rangle dt = \delta_{\alpha,\beta}. \quad (8)$$

In the high frequency region, when A is relatively small and $A/\omega \ll 1$, the adiabatic approximation is met.[18] There is no mixture between different photon modes, since the system needs an energy ω to jump from one photon state to another photon state. Thus, one can only consider the contribution from zero photon state, i.e., $m = m' = 0$, to calculate the matrix elements of the inner product of the Floquet Hamiltonian, $\langle\langle\{n_i\}, m'|H_f|\{n_i\}, m\rangle\rangle = \langle\langle\{n_i\}|H|\{n_i\}\rangle\rangle$. This inner product is determined by the results of the commutation between H and H_e. In our case, the possible nonzero commutation results from the hopping term and the cross Andreev reflection term,

$$\begin{aligned}&\left[\lambda\left(d_1^\dagger d_2 - d_1 d_2^\dagger\right), \mathbf{f}_1(t)\, d_1^\dagger d_1 + \mathbf{f}_2(t)\, d_2^\dagger d_2\right] \\ &= -\lambda A\left(\cos(\omega t) - \cos(\omega t + \vartheta)\right)\left(d_1^\dagger d_2 + d_1 d_2^\dagger\right), \quad (9)\end{aligned}$$

$$\begin{aligned}&\left[\Delta\left(d_1^\dagger d_2^\dagger - d_1 d_2\right), \mathbf{f}_1(t)\, d_1^\dagger d_1 + \mathbf{f}_2(t)\, d_2^\dagger d_2\right] \\ &= -\Delta A\left(\cos(\omega t) + \cos(\omega t + \vartheta)\right)\left(d_1^\dagger d_2^\dagger + d_1 d_2\right). \quad (10)\end{aligned}$$

Therefore, the phase difference ϑ plays a key role in the commutation relation. If $\vartheta = 2k\pi$, for an integer k only the cross Andreev reflection term does not commutate with the driving term. The influence of the driving term then reflects on the matrix elements of the Floquet Hamiltonian through a renormalized cross Andreev coupling $\Delta \to \Delta J_0(2A/\omega)$, where J_0 is the zero-order Bessel function.[21,27] If $\vartheta = (2k+1)\pi$, then the hopping term does not commutate with the driving term and one gets $\lambda \to \lambda J_0(2A/\omega)$. Thus, using the Nambu basis $\Phi = (d_1, d_2, d_1^\dagger, d_2^\dagger)$, the effective Floquet Hamiltonian can be expressed as

$$H_f^{eff} = \frac{1}{2}\Phi^\dagger h_f \Phi + \frac{1}{2}(\epsilon_1 + \epsilon_2), \quad (11)$$

with

$$h_f = \begin{pmatrix} \epsilon_1 & \lambda & 0 & \Delta J_0 \\ \lambda & \epsilon_2 & -\Delta J_0 & 0 \\ 0 & -\Delta J_0 & -\epsilon_1 & -\lambda \\ \Delta J_0 & 0 & -\lambda & -\epsilon_2 \end{pmatrix}, \quad (12)$$

for $\vartheta = 2k\pi$, and

$$h_f = \begin{pmatrix} \epsilon_1 & \lambda J_0 & 0 & \Delta \\ \lambda J_0 & \epsilon_2 & -\Delta & 0 \\ 0 & -\Delta & -\epsilon_1 & -\lambda J_0 \\ \Delta & 0 & -\lambda J_0 & -\epsilon_2 \end{pmatrix}, \quad (13)$$

for $\vartheta = (2k+1)\pi$.

The FPMMFs can emerge by tuning the frequency ω which changes the ratio λ/Δ. When $\epsilon_1 = \epsilon_2 = 0$, a properly tuned frequency makes the ratio $\lambda/\Delta = \pm 1$; or, if we fix the value of λ/Δ first, then, when the zero-order Bessel function equals the value of $\pm\lambda/\Delta$, the solutions of h_f have two degenerated zero energy solutions,

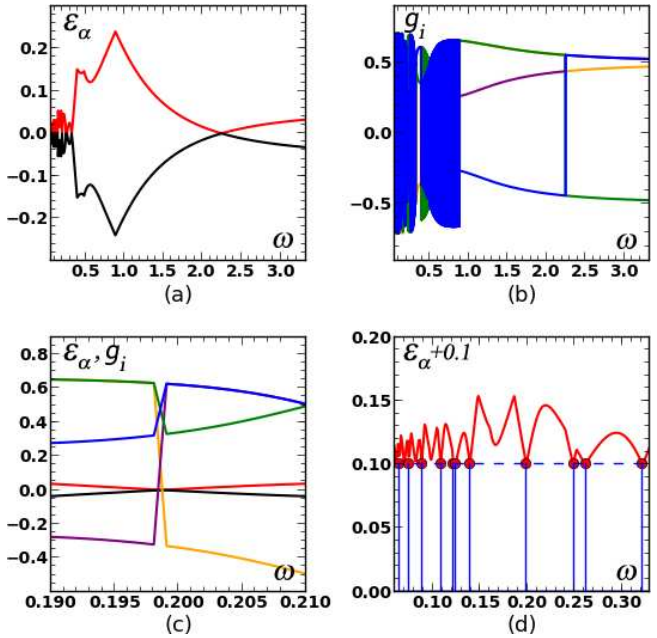

FIG. 3. (Color online) (a) Two quasienergies as a function of ω and (b) the four Floquet modes of the quasienergy (red curve in (a)) as a function of frequency at time zero: the orange curve, green curve, purple curve and blue curve represent g_1 to g_4, respectively. (c) The detailed behaviors of the Floquet modes in the low frequencies when the FPMMFs appear at time zero. (d) Details of quasieneries in the low frequency region, where the red circles represent the FPMMFs emerging. All with a phase difference $2k\pi$.

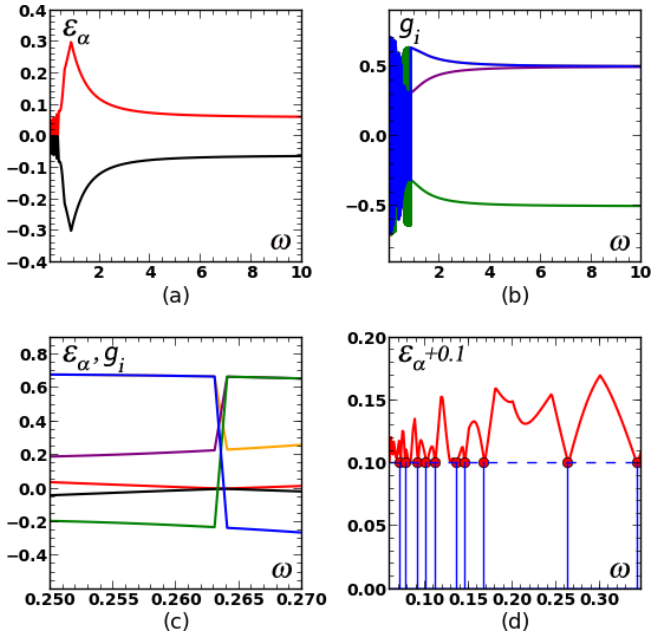

FIG. 4. (Color online) Same with Fig. 3, but all at a phase difference $(2k+1)\pi$. Note that in (b) the orange curve is covered by the blue curve in the high frequency region. Both Fig. 3 and Fig. 4 are calculated in the Nambu space.

$(1,0,1,0)^T$ and $(0,-1,0,1)^T$ for λ/Δ or $(0,1,0,1)^T$ and $(-1,0,1,0)^T$ for $-\lambda/\Delta$. The operator expressions of the Floquet states are $\gamma_1 = (d_1 + d_1^\dagger)/\sqrt{2}$ and $\gamma_2 = i(d_2 - d_2^\dagger)/\sqrt{2}$ or $\gamma_3 = (d_2 + d_2^\dagger)/\sqrt{2}$ and $\gamma_4 = i(d_1 - d_1^\dagger)/\sqrt{2}$, respectively. However, in the high frequency region, one can only find one pair of FPMMFs, γ_1 and γ_2 for example, see the red circle in Fig. 2(a), if one fixed the value of the ratio to $\lambda/\Delta = 0.8$ first. When the phase difference is $(2k+1)\pi$, the inverse of zero-order Bessel function needs to cross the fixed value of the ratio for the FPMMFs to emerge. However, no solutions exist in this case. Therefore, for the same value of the ratio whose $\vartheta = 2k\pi$, changing ϑ to $(2k+1)\pi$ will extinguish the pair of FPMMFs from the quantum dots, see Fig. 2(b).

V. NUMERICAL RESULTS

In this section, we study the low frequency region that is more interesting, though one needs to include the effects of the mixture of the different photon modes. We use the program QuTiP[28] to numerically calculate the quasienergy spectrum both in the high and low frequency region. The QuTiP finds the Floquet quasienergies and modes by calculating and diagonalizing the time evolution operator $U(t_0+T, t_0)$ in Eq. (6).

A. No interaction

We neglect the interaction U and set $\epsilon_1 = \epsilon_2 = 0$, $A = 1$, $\Delta = 0.3$ and $\lambda = 0.24$, then the ratio $\lambda/\Delta = 0.8$, and the numerical results can be compared with the analysis in Sec. IV. It turns out that in addition to confirming the above analysis, in the low frequency region many FPMMFs appear under the condition of both $\vartheta = 2k\pi$ and $\vartheta = (2k+1)\pi$, even though it seems, at the first sight, that the FPMMFs would not emerge in the low frequencies for $\lambda/\Delta = 0.8$ (see Fig. 2(a)). This indicates the contribution of the different photon modes. In Fig. 3(a) and Fig. 4(a), two different quasienergies cross over the zero quasienergy to constitute degenerate states. The Floquet modes at these points constitute the FPMMFs, see the zero time behaviors in Fig. 3(b),(c), and Fig. 4(c). We find that different ratios have different distributions of the FPMMFs in the low frequency region. However, in the high frequency region, when the ratio changes from 0.8 to over 1, the only one pair of the FPMMFs disappear or appear corresponding to the phase difference changing from $2k\pi$ to $(2k+1)\pi$ or vice versa, see Fig. 3(b) and Fig. 4(b). If the energy level in any quantum dot is changed to a nonzero value, the FPMMFs still exist both in the high and low frequencies for $\vartheta = 2k\pi$ and in the low frequencies for $\vartheta = (2k+1)\pi$. Moreover, generally, there are no nonzero quasienergy FPMMFs in this case, since adding or reducing an energy ω will add or reduce a phase with $\exp(i\omega t)$ to the Floquet modes and thus

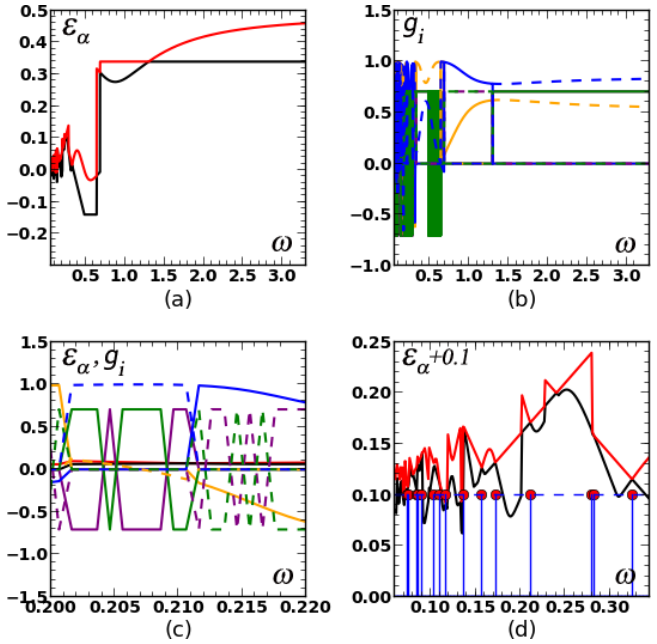

FIG. 5. (Color online) (a) Two quasienergies as the function of ω and (b) the eight Floquet modes of the two quasienergies (red and black curves in (a)) as a function of frequency at time zero: the solid orange, green, purple and blue curves represent g_1 to g_4 of the black color quasienergy, respectively. The dashed orange, green, purple and blue curves represent g_1 to g_4 of the red color quasienergy, respectively. (c) The detail behaviors of Floquet modes in the low frequency when the FPMMFs emerging. (d) Details of quasieneries in the low frequency region, where the red circles represent the FPMMFs emerging.

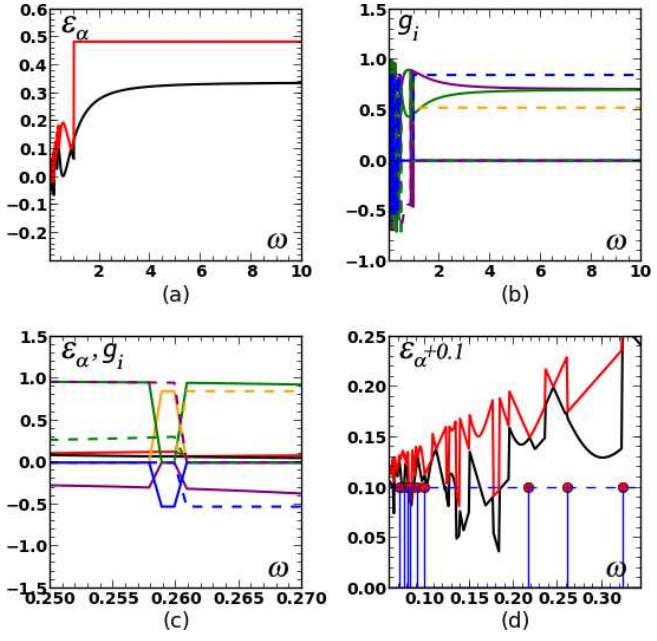

FIG. 6. (Color online) Same with Fig. 5, but all at a phase difference $(2k+1)\pi$. Note that in (b) the solid orange, blue curves and the dashed green, purple curves are overlapped in the high frequency region.

preventing the hermiticity of the Floquet modes from forming the FPMMFs.

For the detail form of the FPMMFs, one can already see in Fig. 3(b) that $g_2(\omega)$ (the green curve) and $g_4(\omega)$ (the blue curve) of the FPMMFs in the high frequency region do not equal zero. So, the operator expression of the FPMMFs do not coincide with $(1,0,1,0)^T$ in the above analysis. This means that there are some overlaps of the FPMMFs locating in different quantum dots, which are (g_1, g_2, g_3, g_4) with $g_1(\omega) = g_3(\omega)$ and $g_2(\omega) = g_4(\omega)$, respectively. Similar behavior shows in the FPMMFs in Fig. 3(c) and Fig. 4(c). This is because the frequencies at which the FPMMFs emerge is not high enough. If we use a larger λ and a smaller A to guarantee the high-frequency FPMMF in Fig. 3(b) appear in a higher frequency region to satisfy the adiabatic approximation, then the Floquet modes will be $(g_1, 0, g_3, 0)^T$ with $g_1 = g_3$. In addition, we note that the only deviation of ϵ_1 away from zero does not change much the frequency of the appearance of the FPMMFs, but the deviation of ϵ_2 from zero at the same time substantially lowers the frequency of appearance of the FPMMFs. Also, $\epsilon_1 \neq 0$ or $\epsilon_2 \neq 0$ makes the overlap of the FPMMFs locate in different quantum dots.

B. With interaction

To consider the interaction effect between the double dots, we change the Hamiltonian from the Nambu space to the Fock space and use the basis $\{|00\rangle, |10\rangle, |01\rangle, |11\rangle\}$, where $|n_1 n_2\rangle$ means having n_1 states in dot 1 and n_2 states in dot 2, respectively. The positions of the four bases correspond to the Floquet modes $\{g_1, g_2, g_3, g_4\}$ in the numerical process. The appearance of FPMMFs now dictates that the Floquet modes with different fermion parity (odd $|\alpha_o\rangle$ or even $|\beta_e\rangle$) have identical Floquet quasienergy. In other words, adding a fermion does not change the quasienergy of the system, which means the FPMMFs have zero quasienergies. The modes are explicitly $|\alpha_o\rangle = (0, g_2, g_3, 0)^T$ with nonzero g_2 and g_3 and $|\beta_e\rangle = (g_1, 0, 0, g_4)^T$ with nonzero g_1 and g_4. We perform numerical calculations in the Fock space. We checked that the results in the Nambu space were reproduced well. We then let ϵ_1, ϵ_2, and U all have nonzero values and find that the FPMMFs still exist, see Fig. 5 at $\vartheta = 2k\pi$ and Fig. 6 at $\vartheta = (2k+1)\pi$ for $\epsilon_1 = \epsilon_2 = 0.1$, $A = 1$, $\Delta = 0.3$, $\lambda = 0.24$ and $U = 0.1$. In Fig. 5(a), two Floquet quasienergies (red and black curves) have a cross point in the high frequency region and many cross points in the low frequency region. At the time zero, the corresponding Floquet modes are shown in Fig. 5(b): g_1 (the solid orange curve) and g_4 (the solid blue curve) of one quasienergy mode and g_2 (the dashed green curve) and g_3 (the dashed purple curve) of the other quasienergy mode become zero while the others become nonzero starting from the high frequency cross point in Fig. 5(a). Thus there is a pair of FPMMFs appears in the cross point.

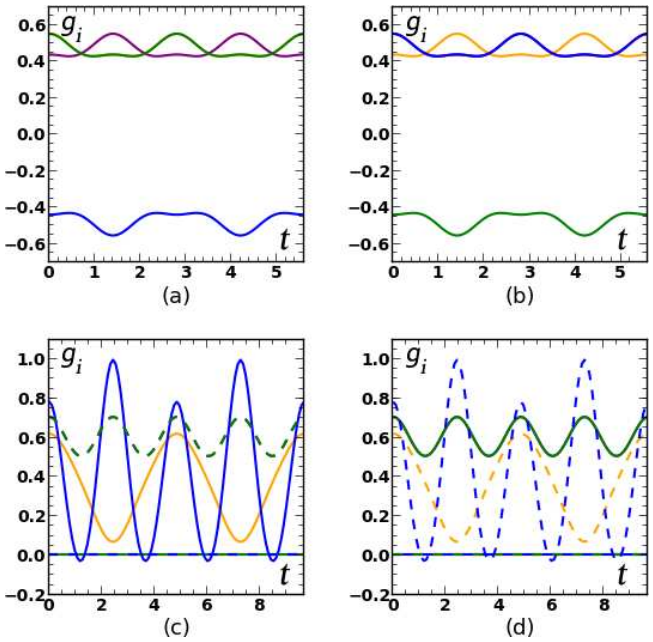

FIG. 7. (Color online) The Floquet modes as a function of the time within two periods. The frequencies of (a) and (b) are the values before and after, respectively, the appearance of the pair of FPMMFs in the high frequency region in Fig. 3. The frequencies of (c) and (d) are the values before and after, respectively, the appearance of the pair of FPMMFs in the high frequency region in Fig. 5

Similar situations happened when the other FPMMFs appear in the low frequencies as indicated by the red circles in Fig. 5(d), see Fig. 5(c) and (d) for details. Note that not all cross points of the red and black curves correspond to the FPMMFs: one can see an example in (d) when the frequency is about 0.24. In a word, the interaction U also supports the existence of FPMMFs, though it lowers the frequency of the appearance of the FPMMFs in the high frequency and changes the distribution of the FPMMFs in the low frequency region.

C. Time evolutions

Note that the Floquet modes shown above are just at the time zero. To see the time evolution of the FPMMFs, we perform numerical calculations using the Floquet modes at time zero as initial states. It turns out that the FPMMFs always exist in the whole time region, see Fig. 7, since the time evolutions of the Floquet modes before and after the frequency at which the FPMMFs appear guarantee that the Floquet modes at the nonzero time behaves similarly to the zero time. It is worth noting that when the adiabatic approximation is met in the higher frequency region, g_2 (the green curve) and g_3 (the purple curve) in Fig. 7(a) will overlap and so will the g_1 (the orange curve) and g_4 (the blue curve) in Fig. 7(b). However, different things happen with the solid orange

and the solid blue curves in Fig. 7(c) and the dashed orange and the dashed blue curves in Fig. 7(d). Since the nonzero energy levels and the interaction lowers the frequency at which the FPMMFs appear, the solid orange and the solid blue curves are hard to overlap and so are the dashed orange and the dashed blue curves. This means they enhance the overlap between the FPMMFs locating in different dots.

VI. SUMMARY

We have introduced the FPMMFs and studied their appearance in the Floquet space. A simple analysis has shown that there is a pair of FPMMFs emerging in the adiabatic approximation when the phase difference in the double dots is the same. Direct numerical calculations have confirmed this analysis and have found a lot of FPMMFs at low frequencies owing to the contributions of different photon modes. Different to other Floquet Majorana fermions, there is no nonzero quasienergy FPMMFs. When the adiabatic approximation is not satisfied even in the high frequency region, there is overlap between the two FPMMFs appearing in the different dots. The nonzero energy levels of the two dots and their interaction do not prevent the emergence of FPMMFs. The different behaviors due to the driving phase difference between the double dots provide a method other than tuning the ratio between the hopping amplitude and cross Andreev reflection amplitude to observe Majorana fermions. The FPMMFs may thus be promising to be found in experiments.

This work was supported by the CNSF (No.10625420) and the FRFCU.

* liyantao@mail2.sysu.edu.cn
† stszf@mail.sysu.edu.cn

[1] C. W. J. Beenakker, arXiv:1112.1950.
[2] J. Alicea, Rep. Prog. Phys. **75**, 076501 (2012).
[3] M. Leijnse and K. Flensberg, Semicond. Sci. Technol. **27**, 124003 (2012).
[4] V. Mourik, K. Zuo, S. M. Frolov, S. R. Plissard, E. P. A. M. Bakkers, L. P. Kouwenhoven, Science **336**, 1003 (2012).
[5] J. R. Williams, A. J. Bestwick, P. Gallagher, Seung Sae Hong, Y. Cui, Andrew S. Bleich, J. G. Analytis, I. R. Fisher, D. Goldhaber-Gordon, Phys. Rev. Lett. **109**, 056803 (2012).
[6] L. P. Rokhinson, X. Liu, J. K. Furdyna, Nature Physics **8** 795 (2012).
[7] M. T. Deng, C. L. Yu, G. Y. Huang, M. Larsson, P. Caroff, H. Q. Xu, Nano Lett. **12**, 6414-6419 (2012).
[8] A. Das, Y. Ronen, Y. Most, Y. Oreg, M. Heiblum, H. Shtrikman, Nature Physics **8**, 887-895 (2012).
[9] J. Liu, A. C. Potter, K. T. Law, P. A. Lee, arXiv:1206.1276.
[10] S. Das Sarma, J. D. Sau, T. D. Stanescu, Phys. Rev. B. **86**, 220506 (2012).
[11] J. Liu, F. C. Zhang, K. T. Law, arXiv:1212.5879.
[12] J. D. Sau, S. Das Sarma, Nature Communications, **3**, 964 (2012).
[13] I. C. Fulga, A. Haim, A. R. Akhmerov, Y. Oreg, arXiv:1212.1355.
[14] D. E. Liu, H. U. Baranger, Phys. Rev. B. **84**, 201308(R) (2011).
[15] J. Alicea, Y. Oreg, G. Refael, F. Oppen, M. P. A. Fisher, Nature Physics **7**, 412-417 (2011).
[16] N. H. Lindner, G. Refael, V. Galitski, Nature Physics **7**, 490-495 (2011).
[17] L. Jiang, T. Kitagawa, J. Alicea, A. R. Akhmerov, D. Pekker, G. Refael, J. I. Cirac, E. Demler, M. D. Lukin, P. Zoller, Phys. Rev. Lett. **106**, 220402 (2012).
[18] G. Liu, N. Hao, S. L. Zhu, W. M. Liu, Phys. Rev. A **86**, 013639 (2012).
[19] A. A. Reynoso, D. Frustaglia, arXiv:1208.2742.
[20] Q. J. Tong, J. H. An, J. Gong, H. G. Luo, C. H. Oh, arXiv:1211.2498.
[21] D. E. Liu, A. Levchenko, H. U. Baranger, arXiv:1211.1404.
[22] L. Hofstetter, S. Csonka, J. Nygård, C. Schönenberger, Nature **461**, 960-963 (2009).
[23] L. G. Herrmann, F. Portier, P. Roche, A. L. Yeyati, T. Kontos, C. Strunk, Phys. Rev. Lett. **104**, 026801 (2010).
[24] M. Leijnse, K. Flensberg, Phys. Rev. B **86**, 134528 (2012).
[25] J. H. Shirley, Phys. Rev. **138**, B979 (1965).
[26] H. Sambe, Phys. Rev. A **7**, 2203 (1973).
[27] A. Eckardt, C. Weiss, M. Holthaus, Phys. Rev. Lett. **95**, 260404 (2005).
[28] J. R. Johansson, P. D. Nation, F. Nori, Comp. Phys. Comm. **183**, 1760 (2012).